

## Article

# Study on the Friction Characteristics and Fatigue Life of Manganese Phosphate Coating Bearings

Lijie Hao <sup>1</sup>, Yong Chen <sup>1,\*</sup>, Guangxin Li <sup>1,\*</sup>, Min Zhang <sup>2</sup>, Yimin Wu <sup>1</sup>, Rui Liu <sup>1</sup> and Guang Chen <sup>1</sup>

<sup>1</sup> Tianjin Key Laboratory of Power Transmission and Safety Technology for New Energy Vehicles, School of Mechanical Engineering, Hebei University of Technology, Tianjin 300130, China

<sup>2</sup> Changzhou NRB Corporation, Changzhou 213000, China

\* Correspondence: chenrong@hebut.edu.cn (Y.C.); 201811201001@stu.hebut.edu.cn (G.L.)

**Abstract:** In this study, the tapered roller bearing was adopted to explore the effect of the manganese phosphate coating on the friction, wear, and lifespan of bearings. Line friction samples with and without a manganese phosphate coating were prepared. The White Light Interferometry was used to analyze the three-dimensional morphology and roughness, and the Optimal Schwing-Reib-Verschleiss-5 multifunctional friction and wear tester was applied to obtain the tribological parameters before and after the application of the manganese phosphate coating. A scanning electron microscopy and energy dispersive spectrometry were used to characterize the microstructure and element composition of the worn surfaces of the manganese phosphate coating. The influence of the manganese phosphate coating on the contact stress was contrasted and examined by establishing a finite element model of the tapered roller bearing. Finally, a life test of the tapered roller bearings was performed before and after the application of the manganese phosphate coating. The results demonstrate that manganese phosphate coating enhances wear resistance, lowers bearing contact stress, and reduces the coefficient of friction. The fatigue life of the tapered roller bearing can be significantly extended with a manganese phosphate coating. This is a new method that can be used to improve the service life of bearings.

**Keywords:** manganese phosphate coating; line friction; micromorphology; finite element; coefficient of friction



**Citation:** Hao, L.; Chen, Y.; Li, G.; Zhang, M.; Wu, Y.; Liu, R.; Chen, G. Study on the Friction Characteristics and Fatigue Life of Manganese Phosphate Coating Bearings. *Lubricants* **2023**, *11*, 99. <https://doi.org/10.3390/lubricants11030099>

Received: 5 January 2023

Revised: 20 February 2023

Accepted: 24 February 2023

Published: 26 February 2023



**Copyright:** © 2023 by the authors. Licensee MDPI, Basel, Switzerland. This article is an open access article distributed under the terms and conditions of the Creative Commons Attribution (CC BY) license (<https://creativecommons.org/licenses/by/4.0/>).

## 1. Introduction

Bearings are an essential part of many types of machinery, including modest domestic items such as air conditioners and refrigerators, as well as vehicles, ships, and airplanes [1]. Bearings are commonly referred to as “meals for the equipment industry”, because they are utilized extensively in numerous mechanical components. Many types of bearings are applied. Among them, rolling bearings are suitable for many different working environments and they have fewer restriction conditions than others. As a result, it is crucial to study the fatigue life of rolling bearings used in machinery. Significant research effort has focused on the development of approaches to prolong the service life of rolling bearings [2,3].

Due to the presence of constant friction during bearing operations, a significant quantity of heat is produced, which increases the temperature of bearings [4]. Previous studies have shown that a significant portion of the failure and destruction of bearing parts occurs on the surface. The processing and manufacturing precision of bearings, the composition of the bearing material, and the heat treatment technology used must all be improved to enhance the performance of bearings. In order to increase the wear resistance of bearings and assure their long-term stable operation, it is necessary to improve the surface qualities of the bearings' component surfaces. In mechanical parts, coating technologies are widely employed to reduce surface friction and improve performance [5].

The reaction principles of phosphating treatment are shown in Figure 1. Eight stages are needed to prepare the manganese phosphate coating. Firstly, the test piece surfaces

are pretreated by degreasing in an alkaline solution at 80–90 °C; secondly, the test pieces are washed with water; thirdly, further treatment is carried out at 50 °C; and finally, phosphating treatment is performed at 90 °C for 10–15 min while maintaining an acid ratio of 5.6–6.2. The following chemical reactions take place during the creation of manganese phosphate coating:

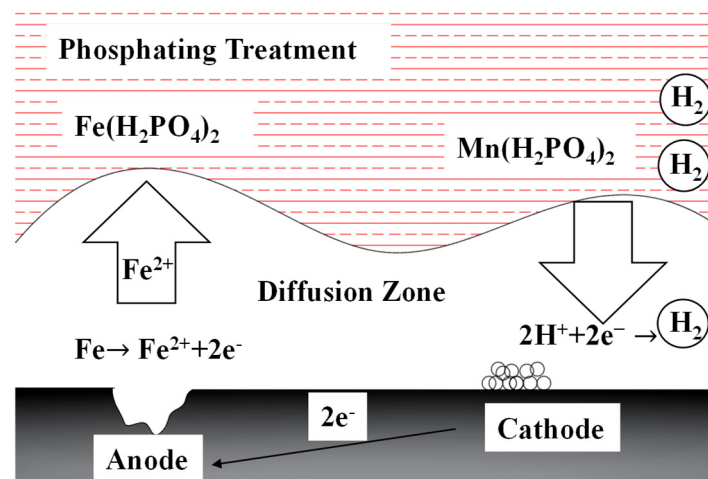


Figure 1. Simplified diagram of phosphating treatment.

After being rinsed with clean water at 20–25 °C, the pieces are dried at room temperature and are then exposed to an oil bath at 20–25 °C, followed by a final 12 h bake in nitrogen at 50 °C.

A manganese phosphate coating was first applied by Koyo Seiko of Japan to improve the lifespan of bearings. The results showed that the ability of bearings with a manganese phosphate coating to form oil film was significantly higher than that of uncoated bearings. The adsorption impact of the manganese phosphate coating structure and lubricating oil layer was investigated by Ernens et al. [6]. The research showed that the manganese phosphate coating forms a friction film during lubrication, which is due to the activation of shear stress. Jia [7] analyzed the wear and friction characteristics of the manganese phosphate coating's gear surface and compared the coefficient of friction before and after the application of the coating. The study confirmed that manganese phosphate coating treatment can reduce the friction coefficient during gear meshing, thus reducing the heat generated by friction during gear meshing. Shi et al. [8] applied a ferrous sulfide coating and manganese phosphate coating to the surface of AISI 5120 steel and analyzed the friction characteristics of the two coatings. The research proved that both coatings have obvious antifriction and wear resistance characteristics; however, with an increase in load, the effect of ferrous sulfide coating on antifriction and wear resistance is not obvious, while the manganese phosphate coating has continuous antifriction and wear resistance characteristics. Ball–disk contact was used by Ilaiyavel et al. [9] to analyze the friction properties of manganese phosphate coatings. It was concluded that the friction coefficient decreases with an increase in load, and the temperature of the manganese phosphate coating is very low after annealing. Olofsson [10] applied an Me-C:H coating to the rollers of tapered roller bearings and carried out a wear test. The results showed that the coating has good wear resistance properties. Zang et al. [11] evaluated the tribological properties of manganese phosphate coatings with a multifunctional friction and wear tester. The results showed that manganese phosphate coating has good antifriction properties, and

the strengthening mechanism of manganese phosphate coatings was investigated from a microscopic perspective.

The lubricating and surface friction characteristics of manganese phosphate coatings were investigated in the aforementioned studies. It has been shown that the application of a manganese phosphate coating to gears can reduce the friction coefficient of the gears' surface, and thus improve the antifriction performance of gears. However, there is a dearth of studies on the effect of manganese phosphate coatings on the lifespan of bearings. In this study, the effects of manganese phosphate on the surface characteristics and lifespan of the tapered roller bearing were explored. The bearings' inner and outer rings were subjected to a manganese phosphate coating. First, the cylindrical and disc samples were manufactured, and then the changes in the coefficient of friction were analyzed using the line contact test. Then, the friction properties of the surface were analyzed before and after manganese phosphate coating and compared by scanning electron microscopy (SEM) and energy dispersive spectrometry (EDS). Finally, the bearing life test was carried out.

## 2. Materials

### 2.1. Disk and Cylinder Substrates

Two sample types were used: A disc with a diameter of 24 mm and a thickness of 7.9 mm and a cylinder with a diameter of 6 mm and a length of 8 mm. The hardness of the samples was 60–65 HRC, and the average roughness was  $R_a = 0.408$ .

### 2.2. Manganese Phosphate Coating Treatment

Manganese phosphate coating was applied to the surface of the base material AISI 52100 steel, and the samples exhibited less surface gloss after treatment with a darker color. The rolling parts of the tapered roller bearings were untreated, but the inner and outer rings were coated with manganese phosphate. When the samples were utilized for friction and wear tests, only the discs were coated. The film thickness of the manganese phosphate coating was about 4.2–5.2  $\mu\text{m}$ , as measured by a high-precision film thickness detector. According to previous research by the current research group, the surface hardness of the thin manganese phosphate coating was determined by the nanoindentation test to be 4.015 GPa. The average surface roughness of the coating sample was  $R_a = 0.408$ .

### 2.3. Lubrication

The lubricating oils used in the SRV test and the tapered roller bearing test were identical to ensure more accurate test results. The lubricating oil parameters are displayed in Table 1. For each set, new samples were used for the test, and before every test, new test samples were added with the same volume of lubricating oil.

**Table 1.** Lubricating oil parameters.

Parameter	L-HM 32
density, $\text{kg}\cdot\text{m}^{-3}$ at 20 °C	854.0
dynamic viscosity, $\text{mm}^2\cdot\text{s}^{-1}$ at 40 °C	32.11
dynamic viscosity, $\text{mm}^2\cdot\text{s}^{-1}$ at 100 °C	5.580
viscosity index	112

### 2.4. Modeling of the Tapered Roller Bearing

In this paper, the tapered roller bearing was chosen as the research object, a three-dimensional model was established in three-dimensional software named Solidworks 2021. The parameters of the tapered roller bearings used in this study are described in Table 2.

**Table 2.** Tapered roller bearing parameters.

Structural Parameters	Parameter Value
external dimensions (mm)	$\Phi 50.8 \times \Phi 92.075 \times 24.608$
rolling body nominal diameter $\times$ length (mm)	$\Phi 9.23 \times 18.07$
number of rolling elements (pcs)	21
pitch diameter (mm)	$\Phi 71.724$
limit speed (rpm)	5600
rated dynamic load $C_r$ (kN)	83.4
rated static load $C_{or}$ (kN)	115.5
inner ring raceway angle	$11^\circ 4'$
rolling body accuracy	Level III
bearing accuracy	Level P0
test radial load (kN)	12.03/19.5
test axial load (kN)	12.63/20

### 3. Methods

#### 3.1. Line Contact Test

The Schwing–Reib–Verschleiss-5 (SRV-5, Optimol Instruments Prueftechnik GmbH, München, Germany) testing machine is a physical performance testing instrument that is used in the field of physics for the friction and wear test. The test device is shown in Figure 2a, and the motion form is shown in Figure 2b. The line contact served as the test's motion form [12]. During the test, the lower sample (disk) is fixed while the upper sample (cylinder) performs a reciprocating sliding friction movement. Before the test, lubricants are injected once through a titration tube into the contact area between the upper and bottom specimens. The load is applied vertically to the disk through the sensor. Taking the bearing of automobile automatic transmission as the research object, the maximum input torque is usually between 250 Nm and 350 Nm. The contact stress is 1000–2500 MPa, taking the working conditions of the bearing test as a reference, combined with standard D7421-11 of the American Society for Testing and Materials (ASTM). Thus, the test loads used were 100 N, 200 N, and 300 N, and the test parameters are provided in Table 3. Each set of testing was carried out three times under the same circumstances to verify the test's reproducibility, and the average coefficient of friction results were computed.

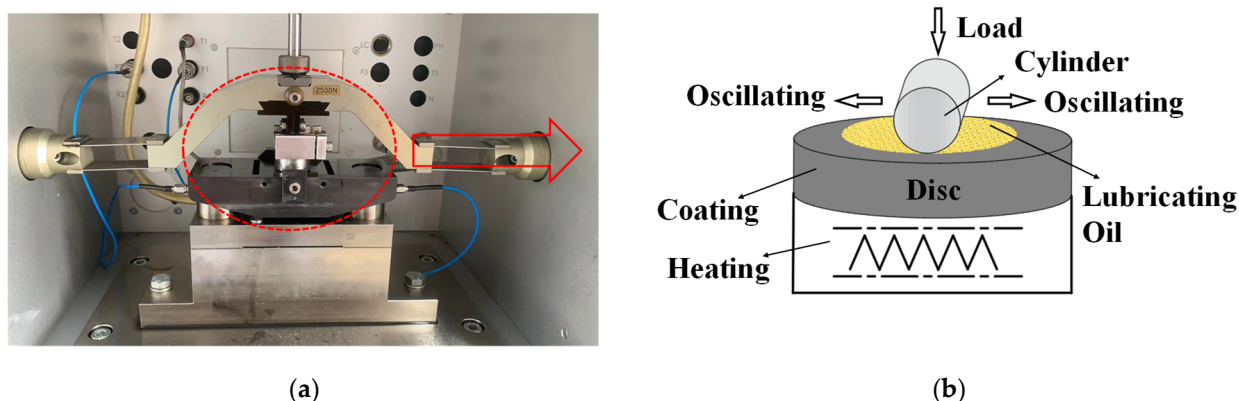


**Figure 2.** Testing principle diagram: (a) testing machine. (b) Principle of motion.

#### 3.2. Surface Morphology Analysis

The White Light Interferometry (Bruker Nano Surfaces, Beijing, China) was used to analyze the three-dimensional (3D) morphology and roughness. SEM (JEOL, akishima, Tokyo, Japan) and EDS (Oxford Instruments, Oxfordshire, England) were used to observe the morphology and composition of the sample's surface before and after the friction and wear test [13].

**Table 3.** Parameters used in the friction experiment.

Test Parameters	Line Contact
load (N)	100, 200, and 300
test time (s)	3600
test temperature (°C)	80
frequency (Hz)	50
sliding speed (m·s <sup>-1</sup> )	0.1
oil volume (ml)	0.3

### 3.3. Calculation of the Contact Stress of the Tapered Roller Bearing

Two revolving bodies with different curvature radii in the main plane come into contact with each other at a point when there is no load, where the upper object is designated as I, and the lower object is designated as II [14].

The curvature sum calculation method is expressed by Equation (4):

$$\sum \rho = \frac{1}{r_{I1}} + \frac{1}{r_{I2}} + \frac{1}{r_{II1}} + \frac{1}{r_{II2}} \quad (4)$$

where  $r$  is the radius of curvature of the raceway groove. Let  $\gamma = D \cos \alpha / dm$ , where  $dm$  is the diameter of the pitch circle of the bearing and  $D$  is the diameter of the roller. When the ball is in contact with the inner raceway, the sum of the curvatures can be obtained by Equation (5):

$$\sum \rho_i = \frac{1}{D} \left( 4 - \frac{1}{f_i} + \frac{2\gamma}{1-\gamma} \right) \quad (5)$$

where  $f = r/D$ , the subscript  $i$  is the inner raceway, and the same is true for the subscript  $i$  below.

Because the roller's contour radius and the raceway groove's radius of curvature are nearly infinite in a tapered roller bearing, the inner raceway's curvature can be calculated by Equation (6):

$$\sum \rho_i = \frac{1}{D_m} \left( \frac{2}{1-\gamma_i} \right) \quad (6)$$

The average diameter of the tapered roller can be obtained by Equation (7):

$$D_m = \frac{1}{2} (D_{max} + D_{min}) \quad (7)$$

where  $D_{max}$  is the diameter of the large end of the tapered roller, and  $D_{min}$  is the diameter of the small end of the tapered roller. The average diameter of the inner ring is taken as the pitch diameter  $d_m$  of the bearing,  $\alpha_i$  is the contact angle of the inner raceway, and  $\gamma_i$  is calculated by Equation (8):

$$\gamma_i = \frac{D_m \cos \alpha_i}{d_m} \quad (8)$$

The radial load  $Q_{ir}$  acting on the bearing will generate loads, as shown in Equations (9) and (10):

$$Q_i = \frac{Q_{ir}}{\cos \alpha_i} \quad (9)$$

$$Q_{ia} = Q_{ir} \tan \alpha_i \quad (10)$$

where  $Q_i$  is the normal load of the roller's inner raceway,  $Q_{ir}$  is the radial load of the roller's inner raceway, and  $Q_{ia}$  is the axial load of the roller's inner raceway.

Hertz's theory assumes that the deformed surface shape is an ellipse of revolution, and an arbitrary function  $V$  is defined by Equation (11):

$$V = \frac{1}{2} \int_{S_0}^{\infty} \frac{(1 - \frac{X^2}{\kappa^2 + S^2} - \frac{Y^2}{1 + S^2} - \frac{Z^2}{S^2})}{\sqrt{(\kappa^2 + S^2)(1 + S^2)}} \kappa dS \quad (11)$$

where  $\kappa = a/b$ ,  $a$ , and  $b$  are the major and minor semi-axes of the projected ellipse of the contact area. For the elliptical contact area, the maximum compressive stress appears at the geometric center, and the magnitude is calculated by Equation (12):

$$\sigma_{max} = \frac{3Q}{2\pi ab} \quad (12)$$

When the compressive stress is distributed as an ideal line contact semi-elliptical cylinder. At point  $\kappa$ , it tends to infinity, and the stress is calculated by Equation (13):

$$\sigma_{max} = \frac{2Q}{\pi lb} \quad (13)$$

For steel bearings, the half-width of the contact surface can be expressed by Equation (14):

$$b = 3.35 \times 10^{-3} \left( \frac{Q}{l \sum \rho} \right)^{\frac{1}{2}} \quad (14)$$

### 3.4. Stress Simulation of the Tapered Roller Bearing

The bearing size barely changes after manganese phosphate treatment. The stress calculated by the aforementioned formula is nearly identical to that of the bearing without a coating; hence, a discernible stress difference between the coated and uncoated bearings cannot be obtained. However, the bearing surface's friction coefficient drastically reduces after coating. In this study, we modified the friction coefficient based on a simulation of the uncoated bearing and then ran the simulation once more to analyze the changes in the stress field of the bearing after coating.

We imported the three-dimensional model into Abaqus 2020 software. We defined the material parameters, and the tapered roller bearing's material characteristics are displayed in Table 4. Tetrahedral meshes were used to divide the components of the tapered roller bearing. The element type was set to a 4-node linear tetrahedron, and the contact area was set to a smaller mesh size. The geometric deviation factor of the mesh was checked and found to be less than 0.2. Finally, 590,415 elements in total were divided [15]. During the simulation, the convergence met the requirements.

**Table 4.** Material properties of the bearing components.

Bearing Elements	Material	Density (kg·m <sup>-3</sup> )	Elastic Modulus (GPa)	Poisson Ratio
inner ring, outer ring, and rolling element	GCr15	7830	219	0.3

Two reference points were selected to set the coupling of the inner ring and the cage, respectively. The interference connections between the rolling elements and the inner and outer ring surfaces, as well as the connections between the rolling elements and the cage pocket surfaces, were established [16]. The surface–surface contact form was used in the simulation analysis. Eighty-four pairs of contacts were established, and the friction factor was set at 0.15. Using the explicit dynamics solver, a linear finite element simulation analysis of a tapered roller bearing was performed.

Firstly, the boundary condition of the bearing outer ring was set to be completely fixed. Next, the inner ring of the bearing was subjected to a speed of 3000 r·min<sup>-1</sup>, and then a

radial load of 12.03 kN and an axial load of 12.63 kN were applied at the coupling point of the inner ring.

The tapered roller bearings experienced a decrease in friction coefficient after being coated with manganese phosphate. We reran the simulation with the friction factor set to 0.145 while maintaining the other conditions.

### 3.5. Life Test of the Tapered Roller Bearing

Structural fatigue characteristics are usually described by the stress-number of the fatigue life cycle curve, as expressed by Equation (15) [17], where  $S$  is the stress,  $S_0$  is the fatigue limit of the material, and  $C$  and  $m$  are the constants of the material.

$$\lg N = \lg C - m \lg(S - S_0) \quad (15)$$

The bearing life test was conducted using type VI bearing life testing equipment. The lubrication method used was oil lubrication. The equipment runs automatically according to the main parameters, such as the preset test load, speed, and running time, and automatically alarms and stops when the set vibration or temperature parameters are reached. The hydraulic progressive loading method was used in this bearing life test to gradually increase the test load. In order to effectively illustrate the influence of manganese phosphate coating on the lifespan of tapered roller bearings and to improve the reliability of the test, low load and high load test conditions were used for two control groups of tapered roller bearings in the life test. The tapered roller bearing type was 28580, and the bearing parameters were the same as those used in the three-dimensional model, as shown in Table 2. The test conditions are shown in Table 5.

**Table 5.** Bearing life test conditions.

Test Conditions	Test Speed (r·min <sup>-1</sup> )	Radial Load (kN)	Axial Load (kN)	Number of Bearings (pcs)	
				Uncoated	Coated
low load	3000	12.03	12.63	2	2
high load	3000	19.5	20	2	2

A thermometer and vibration sensor were used to monitor the temperature and vibration of the outside ring of the test products throughout the test. The vibration sensor was situated between the two stations, and the outer ring of the bearing served as the thermometer's monitoring position. The test temperature was controlled at  $70 \pm 2$  °C, and the maximum test vibration value was twice the vibration value at the beginning of the test. The test equipment was programmed to immediately cease working at a temperature of greater than 95 °C or a vibration measurement that exceeded the maximum limit.

The standards used in this life test were GB/T6391-2010 Rolling Bearings—Rated Dynamic Load and Rated Life and GB/T 24607-2009 Rolling Bearings—Life and Reliability Test and Evaluation.

## 4. Results

### 4.1. Tribological Properties

#### 4.1.1. Coefficient of Friction

The coefficient of friction is depicted in Figure 3a as a time-dependent curve of ordinary heat-treated samples under three loads. During the running-in period, which lasted for the first 300 s of the friction and wear test [18], the friction coefficient changed obviously and started to decrease after a sudden increase. Later, a stable period of friction and wear was reached, where the friction coefficient tended to remain stable. Additionally, the friction coefficient decreased as the experimental load increased.

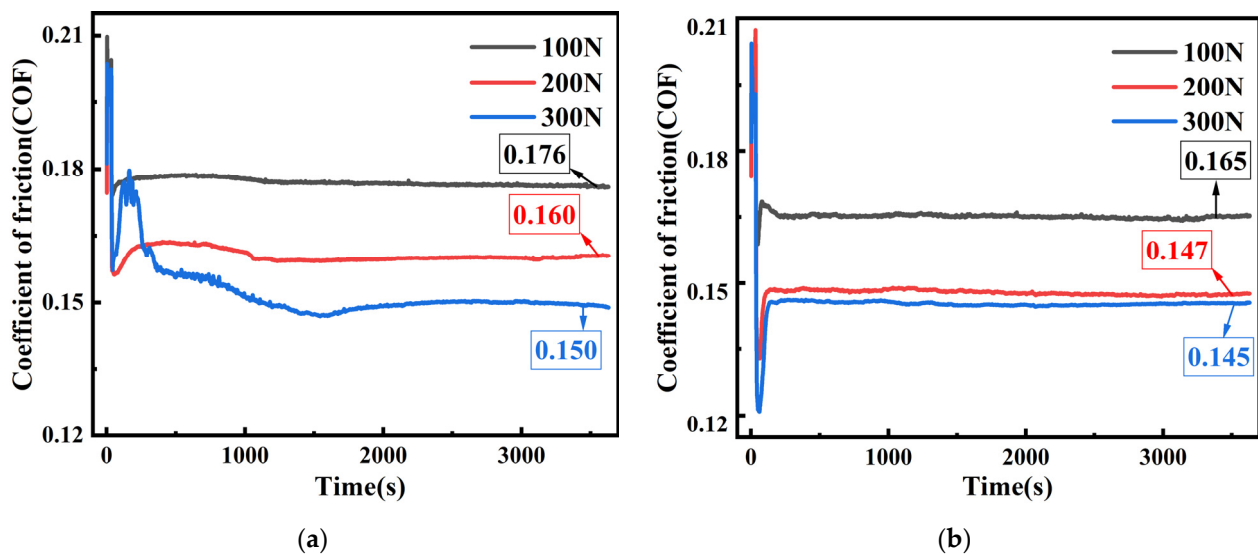


**Figure 3.** The friction coefficients of samples: (a) uncoated; (b) manganese phosphate coating.

Figure 3b depicts the change curve of the friction coefficient for samples coated with manganese phosphate over time and under various loads. When compared with uncoated samples, those with a manganese phosphate coating exhibited more consistent changes in the friction coefficient over time and under three test loads. The friction coefficient of the uncoated sample finally stabilized at 0.150 under a load of 300 N, while the friction coefficient of the sample coating with manganese phosphate stabilized at 0.145.

#### 4.1.2. Surface Roughness

The roughness profile values are displayed in Figure 4a,b. In comparison to the uncoated sample, the surface profile curves following the coating with manganese phosphate exhibited a greater degree of fluctuation. The uncoated sample had a roughness value of  $R_a = 0.124$ , while the sample with coating had a roughness value of  $R_a = 0.408$ . Thus, the roughness value increased. The three-dimensional surface topographies of the uncoated and manganese phosphate coated samples are depicted in Figure 4c,d, respectively. It can be seen that the undulations in the sample's surface were more obvious after coating treatment, indicating that the surface is rougher following treatment with a manganese phosphate coating. This result is consistent with the roughness value shown in the preceding two-dimensional map [19].

#### 4.2. Analysis of the Surface Morphology and Elements

The machining traces on the surfaces of the uncoated samples are depicted in Figure 5a. The sample materials contained high concentrations of C and Fe, as seen in Figure 5b. The manganese phosphate coating's particles are shown to be uniformly distributed in Figure 5c, and the particle size of the coating surfaces indicates that phosphate compounds accumulated on the substrate surfaces. The coating was mostly composed of manganese phosphate compounds with minor amounts of the elements O, P, and Mn, in addition to the components C and Fe, as shown by the energy spectrum analysis presented in Figure 5d.

The surface topography and energy spectrum analysis results of the coated samples obtained after the friction and wear tests under three loads are displayed in Figure 6. It can be seen from the SEM results that there were numerous pits on the surfaces of the samples that can be used to store lubricating oil [20]. Moreover, the sample surfaces were found to have slight scratches as a result of the test, indicating that the manganese phosphate coating exhibits some antifriction activity [21]. Additionally, the worn area was found to have a compacted portion, which implies that the manganese phosphate coating becomes smoother after friction. The results of the energy spectrum analysis presented in

Figure 6b,d,f reveal that the sample surfaces contained P, Mn, and O, suggesting that the samples still had a manganese phosphate coating. The fact that the sample surfaces showed slight signs of wear under the test load of 300 N shows that the manganese phosphate coating continued to have a good solid lubricating effect under a high load.

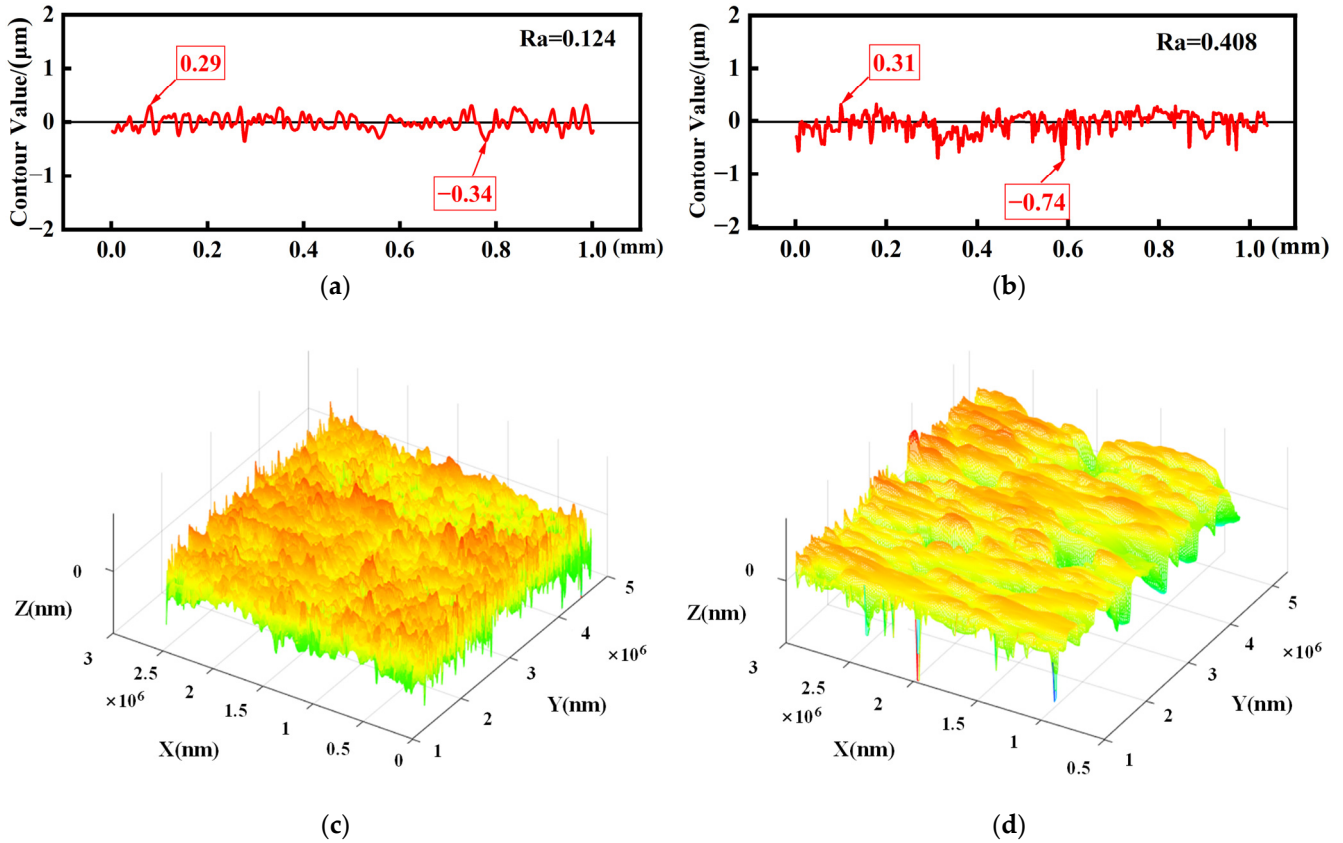


**Figure 4.** Roughness profile values and 3D topography: (a) profile value of uncoated samples; (b) profile value of coated samples; (c) 3D topography of the uncoated samples; and (d) 3D topography of the coated samples.

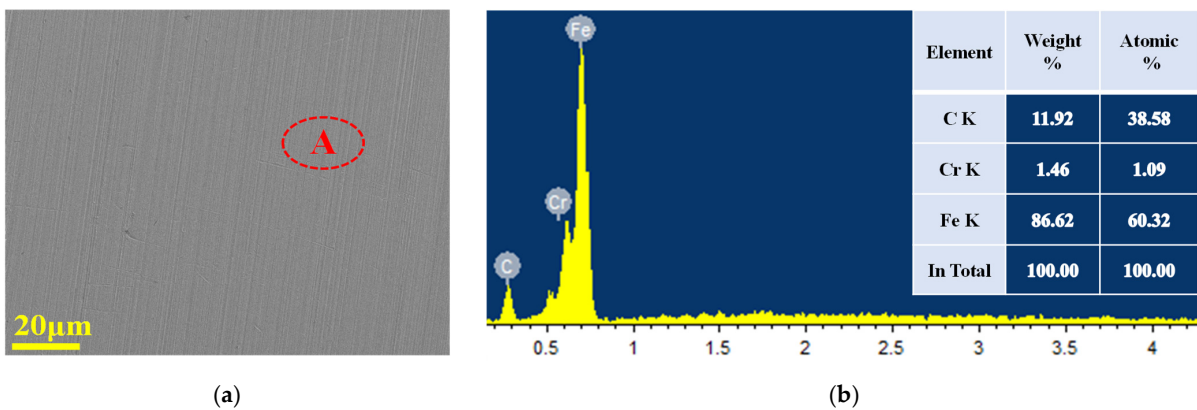


**Figure 5.** Cont.

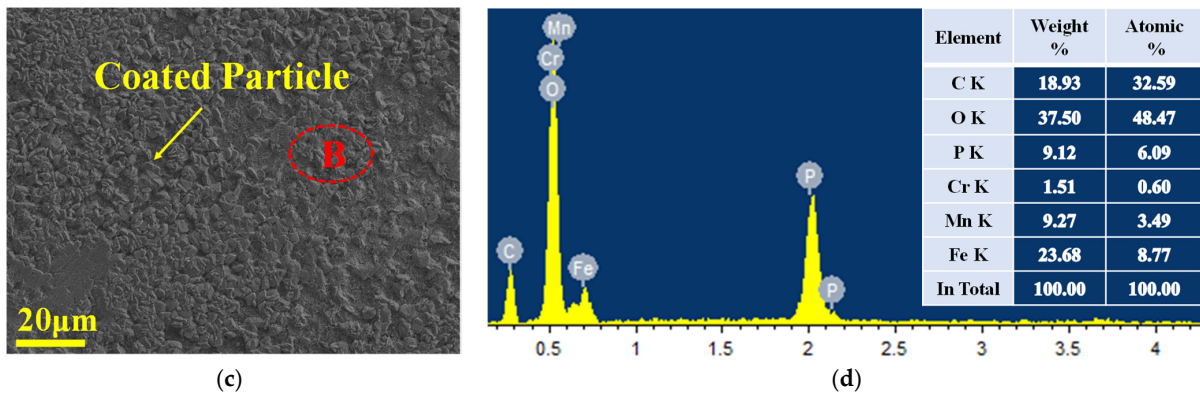


Figure 5. Surface topography and energy spectrum analysis before the wear test: (a) uncoated; (b) EDS spectrum of the A region; (c) manganese phosphate coating; and (d) EDS spectrum of the B region.

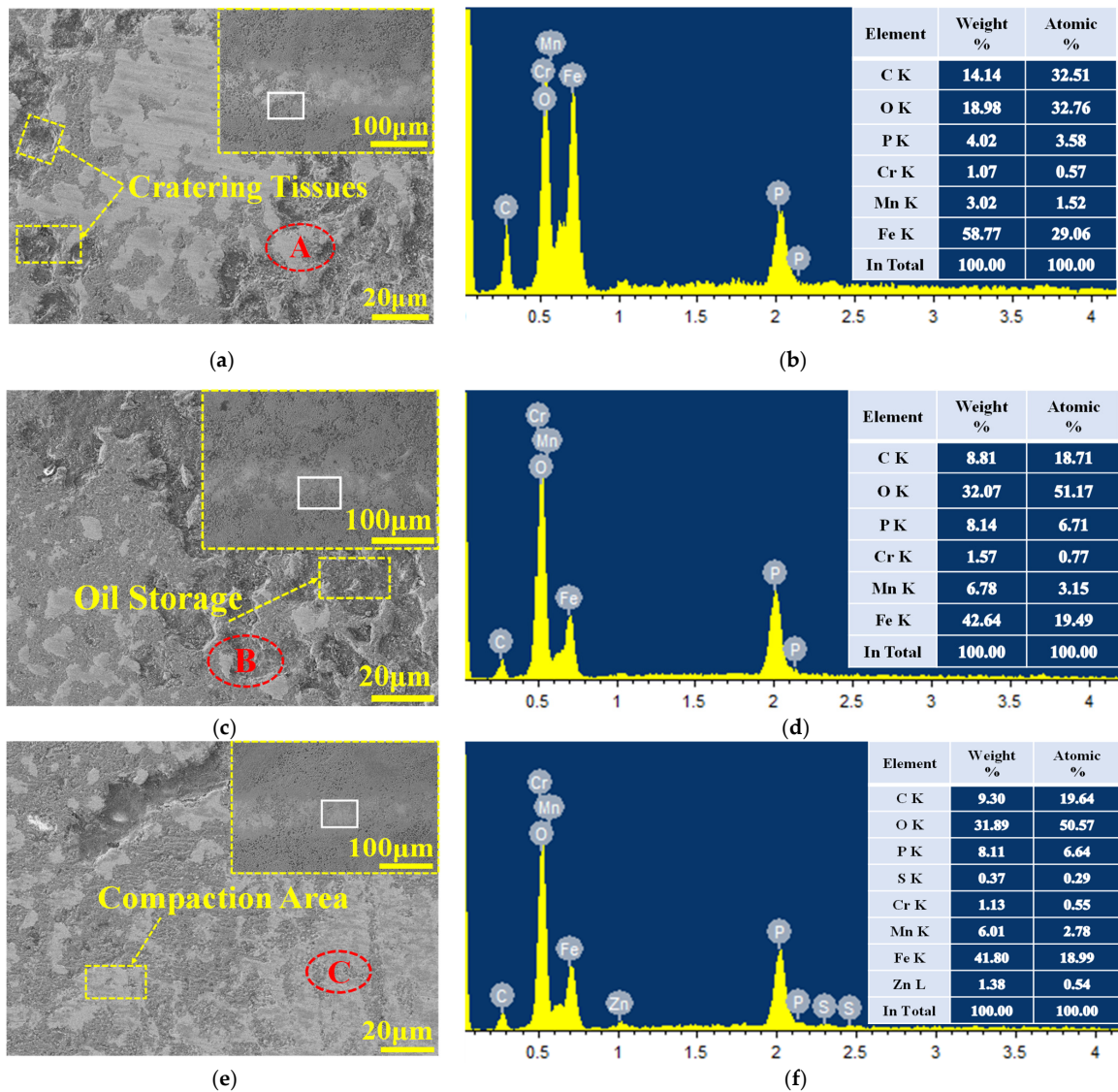
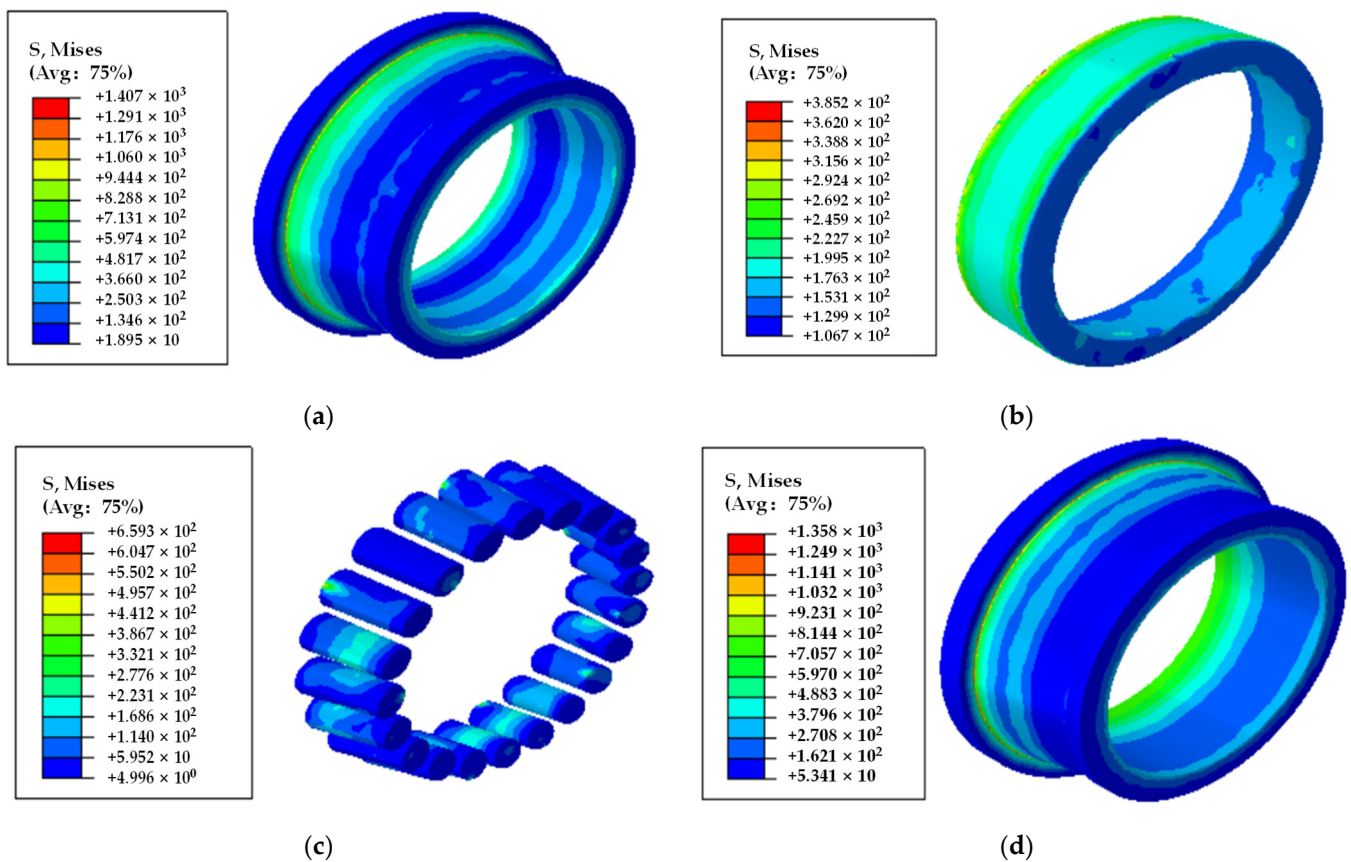


Figure 6. Surface morphology and energy spectrum analysis of samples with manganese phosphate coating after the wear test: (a) wear morphology under a load of 100 N; (b) EDS spectrum of the A region; (c) wear morphology under a load of 200 N; (d) EDS spectrum of the B region; (e) wear morphology under a load of 300 N; and (f) EDS spectrum of the C region.

Surfaces with a manganese phosphate coating have a pit structure that gives them the ability to store oil [22] and allows them to continuously supply lubricating oil between the metals during friction processes. In doing so, wear between the surfaces of the parts is reduced, as is the friction factor.

#### 4.3. Finite Element Simulation

By substituting the test loads and bearing parameters into the above formula, the stress value of bearings under a lower load was found to be 1327 MPa. The inner ring stress of the bearings is demonstrated in Figure 7a and was found to have a size of 1407 MPa. As can be observed from the results presented above, there was a 6.02% deviation between the theoretical and finite element simulation stress values for the bearings. It can be said that the outcome of the simulation is reasonable.



**Figure 7.** Stress cloud diagrams of the tapered roller bearing: (a) inner ring; (b) outer ring; (c) rolling element; and (d) inner ring stress after changing the friction coefficient.

The maximum stress value of the outer ring was 385.2 MPa, and the maximum stress value of the rolling element was 659.3 MPa, as shown in Figure 7b,c, respectively. The stress value of the outer surface of the outer ring was higher than that of the inner surface of the outer ring, because the outer ring of the bearing dissipates heat more efficiently during the operation.

The coated gear was simulated, and the maximum stress value of the inner ring was found to be 1358 MPa, as shown in Figure 7d. Compared with the uncoated bearing simulation, the maximum stress value decreased by 3.48%.

#### 4.4. Life Test of the Tapered Roller Bearing

The failed bearings are shown in Figure 8a,b, respectively. The damaged regions were large and of a bright metallic color. No evident damage was observed outside the damaged areas. Under low-load conditions, uncoated tapered roller bearings one and two operated

for  $3.96 \times 10^7$  r and  $5.94 \times 10^7$  r, respectively, with a pitting failure. After being used for  $3.63 \times 10^8$  r and  $3.45 \times 10^8$  r, respectively, coated bearings one and two experienced pitting failure. The results are shown in Figure 9a. Under high-load conditions, the uncoated bearings ran for  $5.76 \times 10^6$  r and  $4.86 \times 10^6$  r, respectively, and then pitting failure occurred. After being used for  $3.20 \times 10^7$  r and  $3.62 \times 10^7$  r, respectively, the coated bearings failed. The lifespan results are shown in Figure 9b. The results suggest that tapered roller bearings with a manganese phosphate coating have a lifespan that is six–seven times longer than that of uncoated tapered roller bearings.

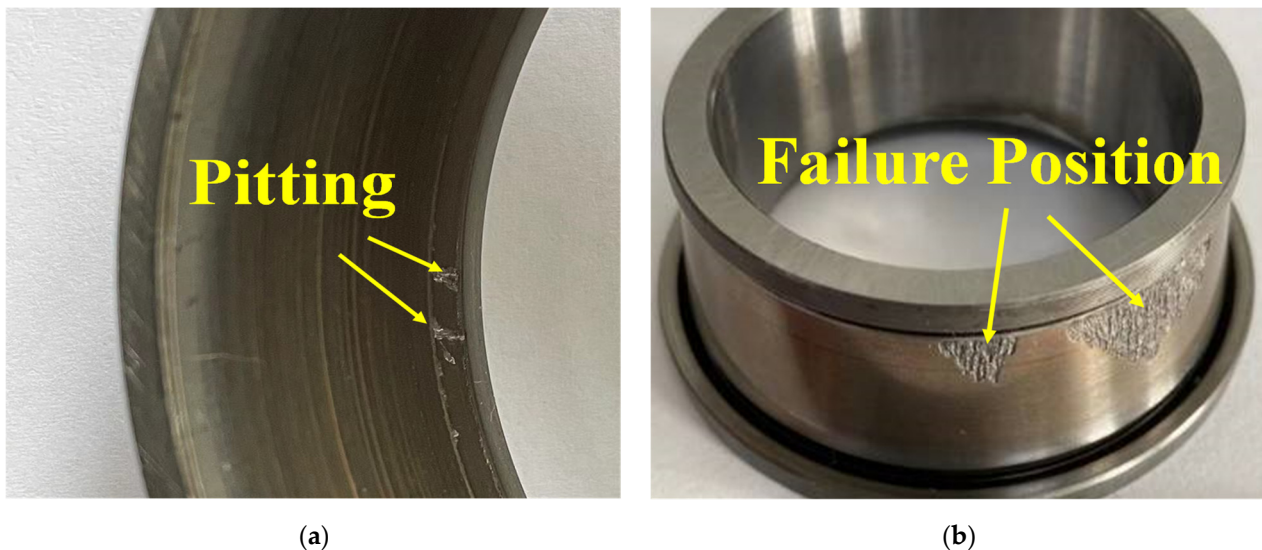


Figure 8. Bearing samples and failed bearings: (a) uncoated invalid bearing; (b) coated invalid bearing.

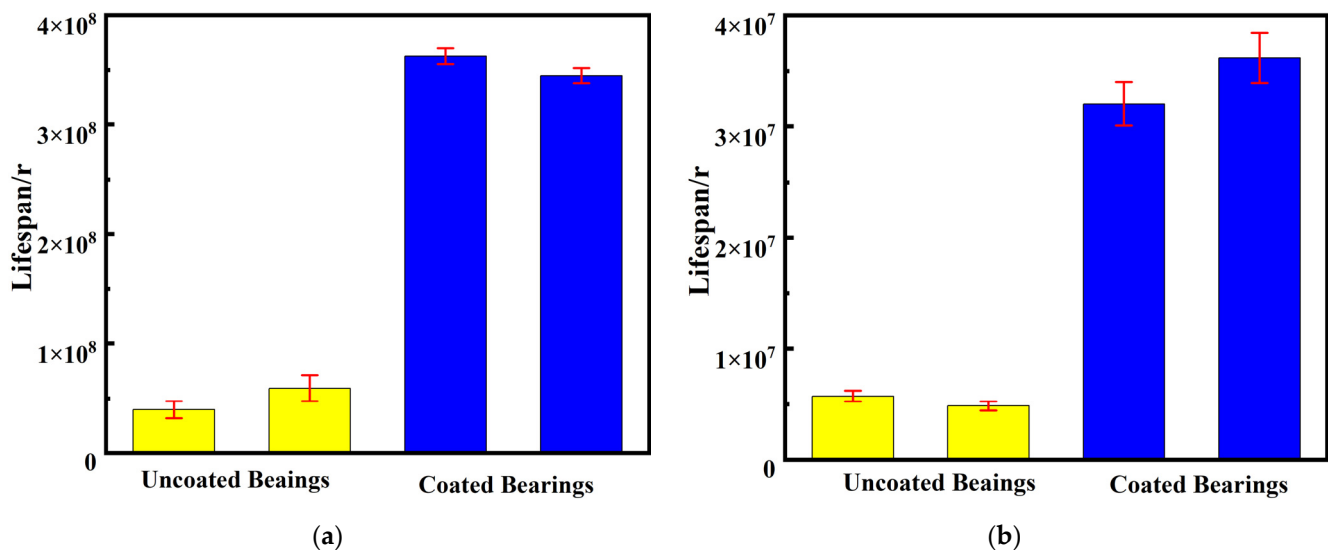


Figure 9. Tapered roller bearing lifespan: (a) bearing life under a low load; (b) bearing life under a high load.

## 5. Discussion

### 5.1. Comparative Analysis of the Friction Coefficient

The comparison of the friction coefficients for test loads of 100 N, 200 N, and 300 N is shown in Figure 10. The friction coefficient decreased by 6.25%, 8.13%, and 3.33% under loads of 100 N, 200 N, and 300 N, respectively. The fact that the sample treated with the manganese phosphate coating exhibited lower friction coefficients than those of

the uncoated sample under the three loads indicates that the coating has a certain level of antifriction activity. Additionally, the bearing lifespan is closely related to contact stress: when the level of stress decreases, the bearing life will increase accordingly.

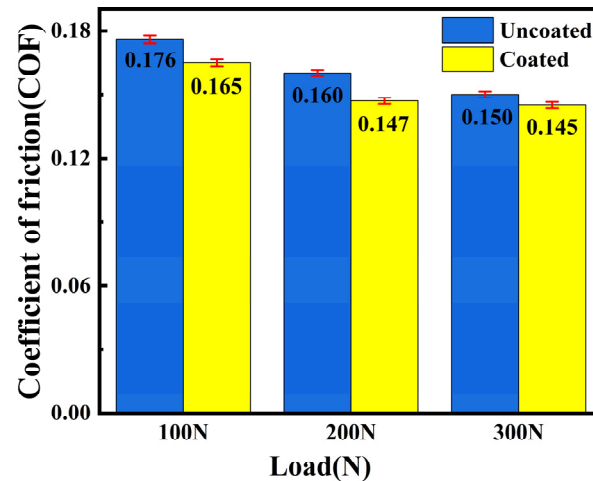
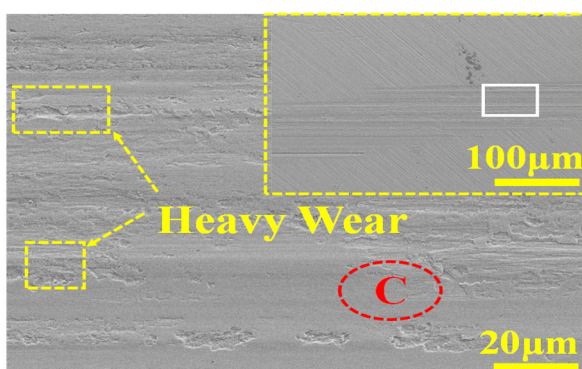


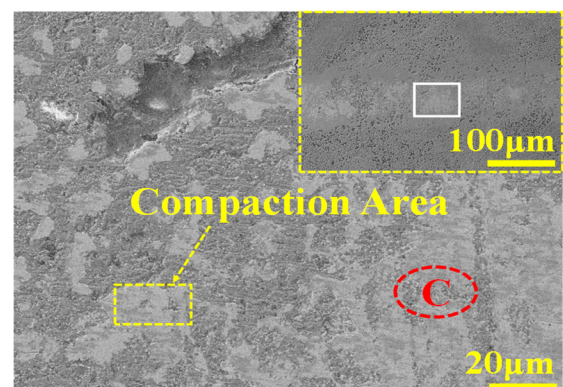
Figure 10. Comparison of friction coefficients.

### 5.2. Wear Mechanism of Manganese Phosphate Coating

The electron micrographs of the uncoated and coated samples after exposure to the 300 N load friction and wear test are displayed in Figure 11a,b, respectively. The surfaces of the uncoated samples in the friction and wear test region were found to have numerous scratches and severe wear, as can be observed from the scanning electron microscope results. However, the surfaces of the samples with the manganese phosphate coating were found to be compacted with slight scratches. As shown in Figure 11c,d, the depth of the wear scar following the friction and wear test of the uncoated sample under a load of 100 N was 0.176  $\mu\text{m}$ . Under a load of 300 N, the scratch depth of the uncoated sample was 0.623  $\mu\text{m}$ , an increase of 0.447  $\mu\text{m}$ , and the rate of growth was 253.97%. The scratches used for the comparison study are depicted in Figure 11e,f. The scratch depth of the coated sample after the 300 N load friction and wear test was 1.12  $\mu\text{m}$  greater in comparison to the depth of the wear mark after the 100 N load friction and wear test. The rate of growth was 18.58%.



(a)



(b)

Figure 11. Cont.

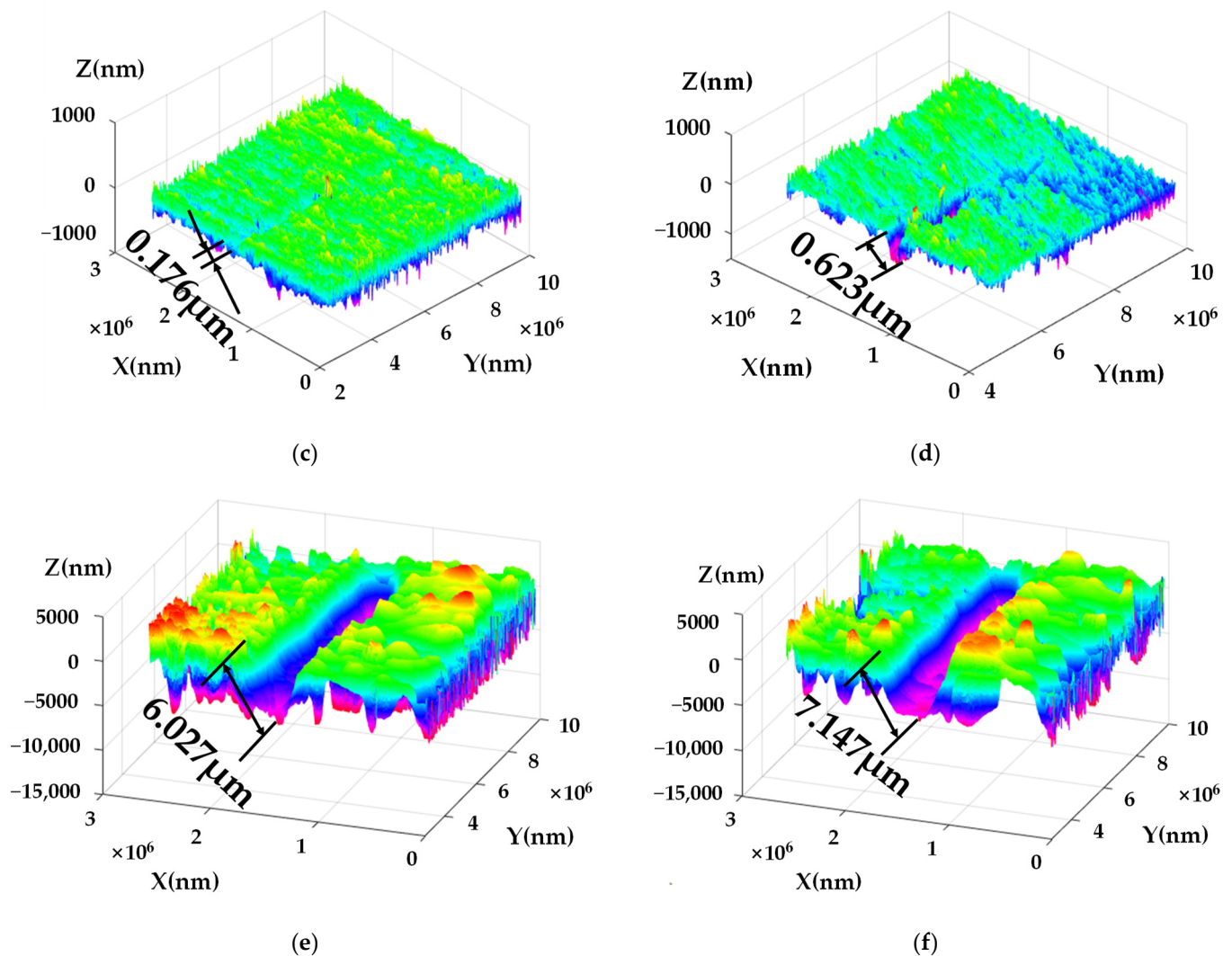


**Figure 11.** Comparison of the SEM and wear scar depth results between the uncoated and coated samples after wear: (a) SEM morphology of the uncoated samples under a load of 300 N; (b) SEM morphology of the coated samples under a load of 300 N; (c) wear scar depth of uncoated samples under a load of 100 N; (d) wear scar depth of uncoated samples under a load of 300 N; (e) wear scar depth of coated samples under a load of 100 N; and (f) wear scar depth of coated samples under a load of 300 N.

In comparison to the uncoated sample blocks, the coated sample blocks exhibited a significantly slower expansion of the wear scar depth. From the above results, it can be concluded that the pits on the manganese phosphate coating's surface can store lubricating oil, minimizing wear and giving the coating a certain degree of abrasion resistance. The wear quantity of the coated sample was greater than that of the uncoated sample, but the growth rate of the wear scar depth was slower than that of the uncoated samples, according to the three-dimensional surface morphology. The sample substrate and the hard layer of the coating became well integrated as the soft layer on the surface wore down, increasing the substrate's ability to resist friction.

### 5.3. Comparative Analysis of Tested Bearings

The dimensions of the tapered roller bearings before and after coating with manganese phosphate are shown in Table 6. The difference in the outer diameter before and after coating was less than 0.01 mm, and the circularity and roughness changed significantly.

**Table 6.** Bearing size changes before and after coating.

External Diameter (mm)		Circularity ( $\mu\text{m}$ )		Roughness Ra ( $\mu\text{m}$ )	
Before Coating	After Coating	Before Coating	After Coating	Before Coating	After Coating
Ø92.097	Ø92.101	1.11	2.79	0.124	0.408

The uncoated and coated bearings under normal load conditions were selected for a comparative analysis, and the results are shown in Table 7.

**Table 7.** Comparative analysis of roughness (Ra) of tapered roller bearing.

Uncoated Bearing ( $\mu\text{m}$ )		Coated Bearing ( $\mu\text{m}$ )	
Before the Test	After the Test	Before the Test	After the Test
0.124	0.117	0.408	0.128

It was discovered, through a comparison of the surface roughness of the coated and uncoated tapered roller bearings before and after the test, that the surface roughness of the coating parts was improved, indicating that the surface coating of bearings can fill the majority of the concave and convex roughness ripples on the bearing surface, and the coating can combine well with the uncoated parts. Moreover, the pit structure on the coating surface can store lubricating oil to allow continuous lubrication during the bearing operation, further reducing the friction coefficient of the bearing surface and promoting the lubrication effect. The table demonstrates that the coated bearings' roughness was still greater than that of the uncoated bearings after the test, indicating that the bearing surface still had a manganese phosphate coating. This is consistent with the SEM results of the coating sample presented in Figure 6 above.

#### 5.4. Scientific Significance and Engineering Value

Gears and bearings have certain similarities in terms of the application of coatings. Firstly, the contact state of the gears and tapered roller bearings is line contact, and the SRV test is line contact. Next, the results of the SRV test and the life test show that coating a gear or bearing with manganese phosphate will reduce the surface friction coefficient and increase the surface resistance to friction as well as the service life. The state of linear contact is slightly different. Gear contact is a sliding motion, while bearing contact is between pure rolling and sliding.

Previous research by scholars concluded that the manganese phosphate coating can reduce the friction coefficient of the part's surface and increase its friction resistance. However, there is a lack of research on the specific effect of the application on bearings. In this study, the characteristics of manganese phosphate coating are obtained by a line contact friction test, which was applied to the bearings and a life test was carried out. This study provides ideas for extending the service life of those parts that are in line contact as well as certain reference values for the application of manganese phosphate coating in line contact. Additionally, effectively prolonging the service life of tapered roller bearings can reduce the operating cost of mechanical equipment. This is of great significance as it could be used to improve the service life of bearings and thus the service life of mechanical equipment.

More bearing samples will be tested in the future to increase the reliability of the test results further, even though existing tests demonstrate that manganese phosphate coating extends the service life of tapered roller bearings efficiently. In the aspect of finite element simulations, it is a kind of exploration to use nonlinear spring elements to simulate the combination of coating and tapered rollers and analyze the changes in the bearing stress field.

## 6. Conclusions

In this study, the effects of manganese phosphate coating on the surface characteristics and lifespan of the tapered roller bearing were investigated. The main conclusions are as follows:

1. Manganese phosphate coating exhibits certain wear resistance properties. The friction characteristics of bearings are similar to those of gears. The surface coefficient of friction can be decreased by coating the tapered roller bearing with manganese phosphate;
2. Manganese phosphate coating can combine well with the substrate. The manganese phosphate coating becomes smoother after friction, as seen by the SEM and EDS results following the line friction test. The pits on the surface of the manganese phosphate coating can store oil to reduce friction;
3. The stress values obtained by the finite element simulation of the tapered roller bearings show that the contact stress decreases after the application of a manganese phosphate coating;
4. The lifespan of the tapered roller bearing can be significantly increased with manganese phosphate treatment, and the lifespan of tapered roller bearings with manganese phosphate coating is six–seven times longer than that of uncoated bearings.

**Author Contributions:** Data curation, L.H., M.Z., Y.C. and G.L.; software, L.H., R.L. and G.C.; writing—original draft preparation, L.H.; writing—review and editing, G.L., Y.C. and Y.W.; project administration, Y.C., G.L. and M.Z. All authors have read and agreed to the published version of the manuscript.

**Funding:** This work is supported by the National Key R&D Program of China (2018YFE0207000).

**Data Availability Statement:** The data presented in this study are available upon request from the corresponding author.

**Acknowledgments:** Hebei University of Technology and Changzhou NRB Corporation are gratefully acknowledged for their support in producing samples and technical services, respectively.

**Conflicts of Interest:** The authors declare no conflict of interest.

## References

1. Hase, A. Early detection and identification of fatigue damage in thrust ball bearings by an acoustic emission technique. *Lubricants* **2020**, *8*, 37. [[CrossRef](#)]
2. Qiu, M.; Niu, K.C.; Li, J.X.; Li, Y.K.; Xu, Y.L. Prediction of remaining life of rolling bearings under multiple stresses. *J. Aerosp. Power* **2022**, *37*, 980–988.
3. Zhong, Z.D.; Zhao, Y.; Yang, A.Y.; Zhang, H.B.; Zhang, Z.H. Prediction of remaining service life of rolling bearings based on convolutional and bidirectional long- and short-term memory neural networks. *Lubricants* **2022**, *10*, 170. [[CrossRef](#)]
4. Winkler, A.; Marian, M.; Tremmel, S.; Wartzack, S. Numerical modeling of wear in a thrust roller bearing under mixed elastohydrodynamic lubrication. *Lubricants* **2020**, *8*, 58. [[CrossRef](#)]
5. Summer, F.; Grün, F.; Ravenhill, E.R. Friction and wear performance of various polymer coatings for journal bearings under stop start sliding. *Lubricants* **2020**, *8*, 1. [[CrossRef](#)]
6. Ernens, D.; Langedijk, G.; Smit, P.; de Rooij, M.B.; Pasaribu, H.R.; Schipper, D.J. Characterization of the adsorption mechanism of manganese phosphate coating derived tribofilms. *Tribol. Lett.* **2018**, *66*, 131. [[CrossRef](#)]
7. Jia, S.; Chen, Y.; Zang, L.B.; Wu, Y.M. Research on temperature field characteristics of gear surface modified based on phosphating coating. *J. Mech. Transm.* **2018**, *42*, 23–26+32.
8. Shi, W.K.; Jiang, H.W.; Qin, D.T.; Chen, Y. Comparison of tribological properties of manganese phosphate coatings and ferrous sulfide coatings. *Mater. Mech. Eng.* **2009**, *33*, 82–85.
9. Ilaiyavel, S.; Venkatesan, A. The wear behaviour of manganese phosphate coatings applied to AISI D2steel subject to different heat treatment processes. *Procedia Eng.* **2012**, *38*, 1916–1924. [[CrossRef](#)]
10. Olofsson, U.; Sjöström, H.; Sjödin, U. Increased wear resistance of roller bearings using Me-C: H coated rollers. *J. Tribol.* **2000**, *122*, 682–688. [[CrossRef](#)]
11. Zang, L.B.; Chen, Y.; Wu, Y.M.; Zheng, Y.; Chen, Y.; You, D.L.; Li, L.; Li, J.K. Comparative tribological and friction behaviors of oil-lubricated manganese phosphate coatings with different crystal sizes on AISI 52100 steel. *Wear* **2020**, *458–459*, 203427. [[CrossRef](#)]
12. Lei, A.L.; Song, X.Y.; Wang, A.X.; Li, X.; Li, X.G.; Zhang, L. Evaluation of friction and wear properties of diesel oil with SRV testing machine. *Lubr. Eng.* **2020**, *45*, 135–140.

13. Zang, L.B.; Chen, Y.; Wu, Y.M.; Liu, H.B.; Ran, L.X.; Zheng, Y.; Gao, M.Z.; Küçükay, F.; Liu, Y.Q. Tribological performance of Mn<sub>3</sub>(PO<sub>4</sub>)<sub>2</sub> coating and PC/MoS<sub>2</sub> coating in Rolling–Sliding and pure sliding contacts with gear oil. *Tribol. Int.* **2021**, *153*, 106642. [[CrossRef](#)]
14. Wang, C.C.; Chen, C.Z.; Wei, Z. Analysis of contact stress characteristics of wind turbine bearings under variable loads. *Noise Vib. Control* **2018**, *38*, 108–111.
15. Liu, J.; Xu, Z.D. A simulation investigation of lubricating characteristics for a cylindrical roller bearing of a high-power gearbox. *Tribol. Int.* **2022**, *167*, 107373. [[CrossRef](#)]
16. Wu, L.; Yao, T.Q.; Fu, Y.N.; Fan, R.R. Dynamic simulation analysis of tapered roller bearing. *J. Kunming Univ. Sci. Technol. (Nat. Sci. Ed.)* **2017**, *42*, 45–50.
17. Qiu, J.; Zhu, R.P.; Lu, F.X.; Jin, G.H. Fatigue life analysis of cylindrical roller bearing based on contact stress. *Mach. Build. Autom.* **2013**, *42*, 18–20+34.
18. Zang, L.B.; Chen, Y.; Ran, L.X.; Jia, S.; Gao, M.Z.; Li, K.; Cao, Z. Experimental study on fatigue characteristics of automatic transmission gears with manganese phosphate coating. *Automot. Eng.* **2017**, *39*, 1203–1210.
19. Zhang, J.W.; Li, W.; Wang, H.Q.; Song, Q.P.; Lu, L.T.; Wang, W.J.; Liu, Z.W. A comparison of the effects of traditional shot peening and micro-shot peening on the scuffing resistance of carburized and quenched gear steel. *Wear* **2016**, *368–369*, 253–257. [[CrossRef](#)]
20. Tamura, Y.; Kobayashi, K.; Aratani, K.; Tanaka, S.; Kikuchi, M.; Masuko, M.; Ohtake, N. Influence of wear surface morphology and Phosphorus-containing tribofilm on crack initiation of manganese phosphate coated steel under Rolling–Sliding contact. *Tribol. Online* **2020**, *15*, 154–169. [[CrossRef](#)]
21. Estupiñan, F.A.; Moreno, C.M.; Olaya, J.J.; Ardila, L.C. Wear resistance of TiAlCrSiN coatings deposited by means of the Co-Sputtering technique. *Lubricants* **2021**, *9*, 64. [[CrossRef](#)]
22. Chen, Y.; Zang, L.B.; Ju, D.Y.; Jia, S. Research status and development trend of surface strengthening technology for high strength automobile gears. *China Surf. Eng.* **2017**, *30*, 1–15.

**Disclaimer/Publisher’s Note:** The statements, opinions and data contained in all publications are solely those of the individual author(s) and contributor(s) and not of MDPI and/or the editor(s). MDPI and/or the editor(s) disclaim responsibility for any injury to people or property resulting from any ideas, methods, instructions or products referred to in the content.